HHS Public Access

Author manuscript

Mol Psychiatry. Author manuscript; available in PMC 2018 September 27.

Published in final edited form as:

Mol Psychiatry. 2018 August ; 23(8): 1773–1786. doi:10.1038/mp.2017.173.

A *Upf3b*-mutant mouse model with behavioral and neurogenesis defects

L Huang[1], **EY Shum**[1], **SH Jones**[1], **C-H Lou**[1], **JN Chousal**[1], **H Kim**[1], **AJ Roberts**[2], **LA Jolly**[3,4], **J Espinoza**[1], **DM Skarbrevik**[1], **MH Phan**[1], **H Cook-Andersen**[1], **NR Swerdlow**[5], **J Gecz**[3,4], **MF Wilkinson**[1,6]

[1]Department of Reproductive Medicine, School of Medicine, University of California, San Diego, La Jolla, California, USA

[2]Department of Molecular and Cellular Neuroscience, The Scripps Research Institute, 10550 North Torrey Pines Road, MB6, La Jolla, CA 92037, USA

[3]School Adelaide Medical School and Robison Research Institute, University of Adelaide, Adelaide, SA 5005, Australia

[4]South Australian Health and Medical Research Institute, Adelaide, SA, 5005, Australia

[5]Department of Psychiatry, School of Medicine, University of California, San Diego, La Jolla, California, USA

[6]Institute of Genomic Medicine, University of California, San Diego, La Jolla, CA

Abstract

Nonsense-mediated RNA decay (NMD) is a highly conserved and selective RNA degradation pathway that acts on RNAs terminating their reading frames in specific contexts. NMD is regulated in a tissue-specific and developmentally controlled manner, raising the possibility that it influences developmental events. Indeed, loss or depletion of NMD factors have been shown to disrupt developmental events in organisms spanning the phylogenetic scale. In humans, mutations in the NMD factor gene, *UPF3B*, cause intellectual disability (ID) and are strongly associated with autism spectrum (ASD), attention deficit hyperactivity disorder (ADHD), and schizophrenia (SCZ). Here, we report the generation and characterization of mice harboring a null *Upf3b* allele. These *Upf3b*-null mice exhibit deficits in fear-conditioned learning, but not spatial learning. *Upf3b*-null mice also have a profound defect in prepulse inhibition (PPI), a measure of sensorimotor gating commonly deficient in individuals with SCZ and other brain disorders. Consistent with both their PPI and learning defects, cortical pyramidal neurons from *Upf3b*-null mice display deficient dendritic spine maturation *in vivo*. In addition, neural stem cells from *Upf3b*-null mice have impaired ability to undergo differentiation and require prolonged culture

Corresponding author: Miles F. Wilkinson: physical address: UCSD, 9500 Gilman Dr., San Diego, CA 92093-0865; phone: (858) 699-4179; no FAX; mfwilkinson@ucsd.edu.

CONFLICT OF INTEREST

The authors declare no biomedical financial interests or potential conflicts of interest.

Supplementary information is available at MP's website.

to give rise to functional neurons with electrical activity. RNA sequencing (RNAseq) analysis of the frontal cortex identified UPF3B-regulated RNAs, including direct NMD target transcripts encoding proteins with known functions in neural differentiation, maturation, and disease. We suggest *Upf3b*-null mice serve as a novel model system to decipher cellular and molecular defects underlying ID and neuro-developmental disorders.

INTRODUCTION

NMD is a RNA degradation pathway initially thought to serve only as a quality control mechanism to degrade aberrant mRNAs encoding potentially deleterious truncated proteins[1]. More recently, NMD has been shown to degrade subsets of normal mRNAs in species spanning the phylogenetic scale[2–7]. Thus, NMD is not only a quality control pathway, but also acts to shape the normal transcriptome. This has led to the hypothesis that NMD regulates normal events, including normal development, which has been supported by many recent studies[3,8–11].

NMD is triggered by in-frame nonsense codons in specific contexts. The best-characterized context that elicits NMD is an exon-exon junction (intron) greater than ~55 nucleotides (nt) downstream of the stop codon defining the end of the main ORF[12]. This "−55 nt boundary rule" is governed by a set of proteins called the exon-junction complex (EJC) that is recruited just upstream of exon-exon junctions after RNA splicing[13]. Evidence suggests that EJCs within the main ORF are displaced by translocating ribosomes, but any that remain downstream of the main ORF can interact with factors recruited upon translation termination, leading to activation of the NMD pathway[13]. It is thought that stop codons less than ~55 nt downstream of the last exon-exon junction fail to trigger NMD because they terminate translation after translating ribosomes displace the most 3′ EJC (given the known length of the EJC and ribosome footpads). Another NMD-inducing feature is a long 3′ UTR, which may elicit NMD by favoring formation of RNA decay complexes over translation complexes[7,14]. Finally, it has been shown that upstream open reading frame (uORFs) trigger NMD under some circumstances, perhaps by virtue of the ability of the stop codon in the uORF to trigger premature translation termination and thereby recruit mRNA decay enzymes[15,16]. To date, the exact mechanisms by which NMD factors are orchestrated to detect these features is unknown.

Several lines of evidence suggest that NMD is not a linear pathway, but rather has different branches. This was first suggested by NMD factor knockdown experiments in HeLa cells. Depletion of EJC factors and the NMD factor, UPF2, selectively upregulated only some NMD substrate RNAs, providing evidence for EJC- and UPF2-independent branches of NMD[17,18]. The existence of a UPF2-independent branch of NMD was later confirmed in *Upf2*-KO mice[19]. The existence of a UPF3B-independent branch of the NMD pathway was initially suggested by two lines of evidence. First, lymphoblastoid cells from patients harboring *UPF3B* frameshifts mutations (that generate premature termination codons) have reduced levels of *UFP3B* mRNA (indicative of active NMD) despite no active UPF3B protein[20]. Second, either stable or transient depletion of UPF3B from HeLa cells failed to reverse the destabilization of a subset of NMD substrates[16]. The existence of both

UPF3B-dependent and –independent branches of NMD was later confirmed *in vivo*[21,22]. NMD branches afford the opportunity for more subtle regulation than regulation conferred by the NMD pathway as a whole. For example, by degrading only a subset of NMD target transcripts, a given NMD branch can influence a given development event in a more specific manner.

Recent genetic studies have revealed that mutations in the *UPF3B* gene cause intellectual disability (ID) in humans[20,23–26]. Mutations in *UPF3B* are also associated with other neurodevelopmental disorders, including autism spectrum disorder (ASD), schizophrenia (SCZ) and attention deficit hyperactivity disorder (ADHD)[23,25,27]. These findings raise the possibility that NMD is important for brain development, a notion supported by recent studies. First, neural differentiation cues trigger NMD downregulation, an event that is sufficient to trigger neuronal differentiation[28]. Second, NMD downregulation is triggered, at least in part, by brain-enriched miRNAs that target the NMD factors UPF1, CASC3, and UPF3B[28,29]. Third, UPF3B is expressed in neural progenitor cells (NPCs) in subventricular zone of developing cortex and its knockdown increases NPC proliferation and reduces their differentiation[3]. These *in vitro* studies support the attractive possibility that NMD and UPF3B functions in neural development but it remains to be determined whether this is the case *in vivo*.

To elucidate the role of UPF3B *in vivo,* we generated *Upf3b*-null mice. We found that these mutant mice have selective defects in behavior that, in part, mimic those found in human *UPF3B* patients. These defects include specific memory and sensorimotor gating deficits accompanied by dendritic spine maturation defects. Cultured mouse neural stem cell (mNSCs) from *Upf3b*-null mice exhibit proliferation and differentiation abnormalities that suggest *Upf3b* functions by promoting neural differentiation. To investigate the underlying mechanism, we performed RNA sequencing (RNA-seq) analysis on *Upf3b*-null vs. control frontal cerebral cortices and identified a remarkably selective set of RNAs dysregulated by loss of *Upf3b*, several of which we found are high-confidence direct NMD targets. Several of these mRNAs encode neural differentiation factors and proteins known to be associated with neuro-developmental disorders. Together, our results suggest *Upf3b*-null mice will be critical for elucidating how abnormalities in post-transcriptional events lead to specific learning and sensorimotor gating defects.

MATERIALS AND METHODS

Cell culture

Gene-trap C57BL6 embryonic stem cell (ESC) clones harboring insertions in the *Upf3b* gene (obtained from the Texas A&M Institute for Genomic Medicine) were cultured as described in our previous study[21]. The IST14619B5 gene trap clone was injected into 6(Cg)-Tyr$^{c\text{-}2J}$/J (albino) donor blastocysts to generate chimeric *Upf3b*-mutant mice, which were bred with C57BL/6J mice to obtain progeny harboring a germline copy of the mutant *Upf3b* (IST14619B5 gene trap) allele. mNSC cultures were maintained and differentiated as described[28]. In brief, mNSCs cultures were isolated from E14.5 *Upf3b*-null and control embryos (n=3 per genotype) and cultured as neurospheres in the presence of EGF and FGF (StemCell Technologies) for 2 weeks before being cryopreserved. Cryopreserved cells

were then thawed and expanded for an additional 3 weeks before experimentation. For multipotent differentiation experiments, neurospheres were expanded in the presence of EGF and FGF to maintain multipotency. Neurosphere cultures (n=3 per genotype) were dissociated into single cells and plated onto ploy-L-ornithine and laminin-coated coverslips (Becton Dickinson and Company). Cells were grown in the presence of EGF for 24 hours before EGF was removed to promote differentiation. Cultures were fixed for analysis 72 hours after plating. Fixed cultures were stained for IF analysis, using standard techniques, employing the following primary antibodies as per manufactures instructions: anti-SOX2 (Millipore, AB5603) anti-GFAP (Sigma, G9269) anti-βIII-TUBULIN (Sigma, T5076). A minimum of 300 cells were scored per culture (n=3 per genotype; SOX2 staining: n=902 control cells, n=990 *Upf3b*-null cells; GFAP/TUBB3 staining: n=904 control cells, n=956 *Upf3b*-null cells). For the EdU pulse-chase experiment, mNSCs were incubated for 48 hours after plating and then labeled with 10 μM EdU (Life Technologies) for 8 hours before being removed and cultured for an additional 24 hours and fixed. EdU was detected using the Clickit-Edu kit (Life Technologies) and immunofluorescently stained using both SOX2 and ant-KI67 (Abcam, ab15580) antibodies. At least 100 EdU-positive cells were scored per culture (n=3 per genotype; SOX2 staining, n=305 control cells, n= =308 *Upf3b*-null cells; KI67 staining, n=306 control cells, n=304 *Upf3b*-null cells). All analyses were conducted blind to genotype. All graphed data points for cell counts represent the mean of n=3 of each genotype (biological replicates) and error bars represent standard deviation. Significance was set at $p<0.05$ using Students two-tailed t-test assuming equal variance. Total cellular RNA was isolated from mNSCs and other cell cultures using Trizol (Thermo Fisher Scientific), as described[29]. For the electrophysiology experiments, directed differentiation of NSC cultures (n=3 per genotype) into pure populations of neurons was conducted as previously described[30]. In brief, neurospheres were dissociated into single cells and plated on multi-electrode array culture plates featuring 64 planar indium tin-oxide (ITO) platinum black electrodes (50 μm × 50 μm electrode size in 8 X 8 rows, with 150 μm spacing). Culture were grown in FGF in the absence of EGF for 1 week to promote expansion of neural-committed mNSCs (over glial-committed mNSCs) before FGF removal to drive neuronal differentiation and maturation. Spontaneous neuron spikes were measured with the integrated MED64 system (Alpha MED Science, Japan).

Mice

Adult C57BL/6 (8- to 11-weeks old) *Upf3b*-null and littermate control mice used for our study. These mice were maintained in agreement with protocols approved by the Institutional Animal Care and Use Committee at the University of California, San Diego. All animals were housed under a 12h light/12h dark cycle and provided with food and water *ad libitum*. Animal procedures comply with the UC San Diego IACUC and ACP standards. Power analyses for behavioral tests were performed on data generated in the Mouse Behavioral Assessment Core examining genotype effects. A simple calculator (http://powerandsamplesize.com/Calculators/) that uses effect size, n, and p = 0.05 significance level was used. Y-maze alteration: N = 14, power = 0.96; Barnes maze test: N = 12, power = 0.72; acoustic startle, PPI: N = 8, power = 0.92; cued and contextual fear conditioning: N = 10, power = 0.97; EEG studies (sleep, auditory brainstem response): N = 6, power = 0.82. Sample sizes were estimated based on power analyses of past similarly designed

studies. None of the samples or animals was excluded from analyses. All animals were treated identically. Male mice were always tested prior to females; mice within a cage were randomly assigned numbers so that the different genotypes were randomly ordered. The experimenters were blinded to genotype throughout testing and initial analyses and were only unblinded at the time of graphing and statistical analysis. All mice were assigned a discreet number that was used to track them throughout experimentation and this number was not associated with a genotype until unblinding. The behavioral data were normally distributed and variances were similar between groups to be compared, therefore parametric statistical tests were justified and used.

Protein analysis

For Western blot analysis, adult female wild-type and *Upf3b*$^{-/-}$ brains were isolated, chopped into small pieces, and placed into a RIPA lysis buffer (Sigma) containing phenylmethane sulfonyl fluoride for 30 minutes on ice to lyse cells and release proteins. Protein concentration was calculated using a DC BSA assay (Bio-Rad Laboratories) and Western blotting was performed as described previously[28]. For immunohistochemistry, adult male wild-type and *Upf3b*-null brains were isolated and immediately placed into optimal-cutting temperature (OCT [Sakura]) solution and frozen for cryosectioning. Cryosectioning was done at 12 μm thickness using a Leica 1500 machine and tissue sections were placed on Superfrost microscope slides (Fisherbrand) and stored at −80C until ready for use. At the time of staining, the sections were air-dried for 20 min, followed by incubation with 4% paraformaldehyde (Electron Microscopy Sciences) for 10 min to fix the tissue. After PBS washes, the sections were permeabilized with 0.1% Triton-X 100 for 10 min. The subsequent staining procedures were done as previously described[29]. mNSCs immunohistochemistry was performed as described previously[31]. Microscopy analysis was performed using a Leica AF6000 epi-fluorescence microscope.

Behavioral analyses

In all assays, *Upf3b*-mutant and wild-type littermates were compared. Prepulse inhibition (PPI) testing was performed as described in a previous study, using startle chambers to produce high-frequency acoustic stimuli[32]. Locomotor, light/dark transfer, cued and contextual fear conditioning, and Barnes maze test were performed as previously described[33]. Y maze and paw clasping behavior were performed as described previously[34].

Golgi staining of neurons and dendritic spine analysis

Golgi staining was performed using the FD Rapid GolgiStain Kit (FD Neurotechologies). In brief, freshly dissected brains were immersed in the impregnation solution for 3 weeks in the dark and cryopreserved. Sections were cut to 0.1 mm thickness and placed on gelatin-coated microscope slides and stained according to the manufacturer's protocol. Imaging of dendritic spines was performed using the BioRad Radiance 2000 laser scanning, brightfield upright confocal microscope. Dendritic spine counting was done using ImageJ and Cell Counter plug-in script.

RNAseq analyses

RNA was isolated from five *Upf3b-null* frontal cortices and six wild-type mouse frontal cortices with the Direct-zol RNA MiniPrep Plus Kit (Cat. R2072; ZYMO Research), quality evaluated by TapeStation (Agilent), and sequenced with an Illumina HiSeq 4000 High-Throughput Sequencing System. Libraries were constructed and reads mapped with the RNA-seq aligner STAR[35,36]. Counts for each gene were quantified using the python script rpkmforgenes.py[37] and annotated using the Refseq mm10 genome. Reads were filtered, such that genes without at least one sample with at least 10 raw reads and one RPKM reads were removed from the analysis. Overlapping RefSeq transcripts were collapsed giving one expression value per gene locus. The count data was normalized and differential expression was performed using the R (v.3.1.1) package DESeq2 (v.1.4.5). In brief, DESeq2 uses negative binomial generalized linear models and shrinkage estimation for dispersions and fold changes to improve stability and interpretability of the estimates. It reports a P value and an adjusted P value using the Benjamini–Hochberg procedure. Genes with an adjusted P value <0.05 were considered differentially expressed unless otherwise noted. Other plots were constructed using the R(v.3.1.1) package gplots. All functional enrichment analyses were generated using DAVID gene annotation and analysis resource[38,39]. For analysis of NMD-inducing features, corresponding Refseq transcripts were converted into Ensemble transcript IDs and sequences were obtained using the UCSC Table Browser. To identify NMD-inducing features, we used a script developed by the laboratory that was previously published[40]. Transcripts defined as having NMD-inducing features have either a ≥1200 nt 3′UTR, a stop codon defining the main ORF >55 nt upstream of at least one exon-exon junction, or an uORF at least 30 codons long defined by an ATG in a Kozak context. Only Ensembl-defined transcripts harboring both 5′UTR and 3′UTR regions were considered for analysis.

RESULTS

Generation of *Upf3b*-null mice

To generate *Upf3b*-mutant mice, we first screened two ESC clones harboring gene trap insertions for *Upf3b* expression. One ESC clone had the cassette insertion in intron 1 (IST14619B5) and the other in intron 4 (IST10135A8) (Supplementary Figure S1a). In both clones, use of the splice accepter (SA) sequence in the cassette leads to the generation of a fusion transcript predicted to encode a truncated form of UPF3B protein. We analyzed the expression level of these two ESC clones and found that clone IST14619B5 had >90% reduced level of *Upf3b* mRNA relative to that in control ESCs, whereas clone IST10135A8 exhibited only a ~50% reduction in *Upf3b* mRNA levels (Supplementary Figure S1b). Of note, the reduction in *Upf3b* mRNA level is likely to be an underestimate, as there were probably some feeder fibroblasts (which express wild-type *Upf3b*) still remaining, even though we passaged the ESCs 3 times in the absence of fresh feeder cells.

We selected the IST14619B5 clone to inject into donor blastocysts for the generation of chimeric *Upf3b*-mutant mice. Following breeding for germline transmission of the mutant *Upf3b* gene, we obtained global *Upf3b*-mutant mice, which were normal in appearance and were viable and fertile. *Upf3b* mRNA levels were decreased by >100-fold in most tissues,

and NMD substrates were upregulated, as reported previously[21]. To determine whether protein expression of UPF3B is also extinguished in these mice, we performed Western blot analysis and found that UPF3B protein was undetectable in brains from *Upf3b*-mutant mice, whereas it was abundant in control brains (Supplementary Figure S1c). Immunofluorescence analysis also showed absence of UPF3B in the brain, including the hippocampus and cerebral cortex (Supplementary Figures S2a & S2b). We conclude that the mutant mice we generated lack detectable UPF3B and thus we will refer to them as *Upf3b*-null mice.

Behavioral analysis of *Upf3b*-null mice

Given that humans with *UPF3B* mutations invariably exhibit intellectual disability and also often suffer from neuro-developmental disorders (see Introduction), we performed behavioral tests on male and female *Upf3b*-null mice. For females, we compared complete KO ($Upf3b^{-/-}$) and heterozygotes ($Upf3b^{+/-}$) with littermate controls ($Upf3b^{+/+}$). For males, we compared only KO ($Upf3b^{-/Y}$) with littermate controls ($Upf3b^{+/Y}$), as *Upf3b* is a X-linked gene. We performed our initial analysis on both sexes together and thus analyzed only *Upf3b*-null and wild-type mice. Later, we analyzed the 3 genotypes separately in females to determine whether there was an effect of heterozygosity.

A general health, sensory, and neurological screen revealed that *Upf3b*-null mice were not significantly different from controls in most respects. For example, *Upf3b*-null mice did not have a significant vision deficit, as determined using the optomotor test (Supplementary Figure S3a). *Upf3b*-null mice also performed normally in the light/dark transfer test of anxiety-like behavior[41] and in a locomotor activity test in which ambulatory, center, and rearing activity is recorded (Supplementary Figures S3b & S3c). The only motor defect we observed in *Upf3b*-null mice was paw-clasping behavior (Supplementary Figure S3d), a trait relatively common in mouse models of several neurological disorders, including Alzheimer's disease, Rett's syndrome, and Huntington's disease[42]. In this test, mice are picked up by the distal third of their tails and observed for 10 sec to determine if they clasp their front paws.

Upf3b-null mice have cued and contextual fear learning defects

Given the paw-clasping trait observed in *Upf3b*-null mice and the fact that *UPF3B* mutations in humans cause ID (see Introduction), we next assessed whether *Upf3b*-null mice have learning defects. We observed no significant effects of genotype (or sex x genotype interactions) in either the Y maze test (Supplementary Figures S4a & S4b) or the Barnes maze test (Supplementary Figures S4c & S4d), which measure simple working memory and spatial learning/memory, respectively. In striking contrast, *Upf3b*-null mice had deficits in both contextual and cued fear conditioning (Figures 1a & 1b). Examination of the context test using repeated measures analysis of variance (RMANOVA; habituation vs. context exposure) in male and female *Upf3b*-null and control mice revealed significant genotype effects ($F[1,47] = 5.5$; $p < 0.05$) and genotype x test effects ($F[1,47] = 6.7$; $p < 0.05$), with no difference between sexes. *Upf3b*-null mice also showed decreased freezing in the context test relative to wild-type mice ($F[1,47] = 6.1$; $p < 0.05$). Examination of the cued test (pre-cue exposure vs. cue exposure) also revealed significant genotype effects ($F[1,47] = 19.5$, $p < 0.0001$) and genotype x test effects ($F[1,47] = 19.0$, $p < 0.0001$). *Upf3b*-null

mice showed decreased freezing in the cued test relative to wild-type mice (F [1,47] = 19.9, p <0.0001). In females, there was a significant effect of genotype x test in the cued test (RMANOVA pre-cues vs. cue exposure; (F [2,34] = 5.0, p <0.05) with the Fisher's PLSD post-hoc testing revealing a difference between *Upf3b*-null and control mice during cue exposure. Heterozygotes exhibited an intermediate response. Together, these data suggest UPF3B is specifically critical for both contextual and cued fear-based learning, but not for simple working memory or spatial learning and memory.

Sleep alterations in *Upf3b*-null mice

We observed that *Upf3b*-null mice also exhibited abnormal sleep behaviors. RMANOVA analysis of male and female *Upf3b*-null and control mice revealed significant overall genotype differences in time spent awake (KO>WT; F [1,25] = 8.3; p <0.01), in slow wave sleep (WT>KO; F [1,25] = 5.7; p <0.05), and in rapid eye movement (REM) sleep (WT>KO; F [1,25] = 14.6; p <0.001) (Figure 1c). Deeper analyses showed that *Upf3b*-null mice had more episodes of these vigilance states than control mice, but that the average episode durations were shorter (data not shown). When females were analyzed separately this genotype effect did not reach significance (Figure 1d). This was likely due to a slight increase in variance with fewer mice included and not due to a sex difference as there were no overall sex differences in vigilance states. There were significant sex x light phase interactions in all vigilance states, but no interactions of genotype x sex or 3-way interactions (Figure 1d and data not shown).

Upf3b-null mice exhibit startle reflex and PPI deficits

The startle response is a largely automatic defensive response to sudden stimuli. Given that the startle response is deficient in several mouse models of human neural diseases[43], we examined *Upf3b*-null mice for this behavior. We found that *Upf3b*-null males and females exhibited a statistically significant deficiency in the magnitude of the acoustic startle response to 90 — 110 dB(A) pulse intensities (Figure 2a). Their deficiency was specific to low intensity pulses, as they responded normally to 115 and 120 dB(A) pulses. RMANOVA analysis of *Upf3b*-null and WT genotypes of both sexes revealed a significant interaction of genotype x pulse intensity (p <0.002). *Post hoc* analysis by Fisher PLSD testing confirmed reduced acoustic startle magnitude in *Upf3b*-null vs. control mice for weaker (90 – 100 dB[A]) pulse intensities (P ≤0.001 for all magnitudes). Female-specific analysis detected a similar interaction of genotype x pulse intensity (p <0.05), with reduced acoustic startle magnitude in *Upf3b*-null vs. both WT and heterozygous mice for 90–95 dB(A) pulses (p <0.02 – 0.05), and vs. heterozygotes for 100–110 dB(A) pulses (p <0.05) (Figure 2b). Deficits in acoustic startle magnitude were not evident in mutants with a 120 dB(A) pulse and thus this magnitude pulse was subsequently used to measure PPI (below). Analyses of reflex habituation (reduction in startle magnitude from the initial to final trial blocks) revealed habituation but no consistent effects of genotype (data not shown).

Prepulse inhibition (PPI) is an operational measure of sensorimotor gating defined as a reduction in startle magnitude when the startling pulse is immediately preceded by a weak prepulse[43,44]. Given that human schizophrenia patients exhibit deficient PPI[43,45] and humans with *UPF3B* mutations often manifest symptoms of SCZ and other neuropsychiatric

disorders associated with impaired PPI[25,27,46], we elected to examine PPI of *Upf3b*-null mice. We found that *Upf3b*-mutant mice had a profound defect in PPI. RMANOVA analysis and *post hoc* Fisher PLSD testing of *Upf3b*-null and WT genotypes of both sexes revealed a significant effect of genotype, when PPI was tested using 100 ms prepulse intervals (gap from prepulse onset to pulse onset) and three prepulse intensities (Figure 2c), and when PPI was tested using a single 85 dB(A) prepulse intensity and 25 – 500 ms prepulse intervals (Figure 2d) (both comparisons: *Upf3b*-null < WT; $p < 0.0001$). Analyses of only females detected a similar effect of genotype across both prepulse intensities and intervals ($p < 0.0006$ and < 0.0007, respectively), with comparable PPI deficits evident in both *Upf3b*-null and heterozygous female mice (Figures 2e & 2f). Analysis of startle magnitude revealed no significant main or interaction effects of genotype or sex (data not shown). This confirms that the observed PPI deficits did not reflect potentially confounding group differences in startle magnitude. We note that deficient PPI and acoustic startle magnitude in *Upf3b*-null mice could not be explained by primary deficits in auditory sensitivity, as these mice exhibited normal auditory sensitivity in measures of auditory evoked potentials (see below).

PPI is regulated by a distributed neural circuitry, with a prominent role of forebrain dopamine activity[47]. To test whether loss of *Upf3b* acts by perturbing dopamine signaling, we elected to test the effect of the potent dopamine D2-receptor antagonist, haloperidol. We found that haloperidol did not have a significant effect on either the startle magnitude or PPI defects in *Upf3b*-null mice (Supplementary Figure S5), providing evidence against this hypothesis.

To test the possibility that both reduced acoustic startle magnitude and reduced PPI in *Upf3b*-null mice reflects a loss of auditory sensitivity or processing, we measured the auditory evoked potential (AEP) response in *Upf3b*-null and WT mice. Brain stem potentials were measured at four decibel levels (65, 68, 70, and 80 dB) and latencies and amplitudes of the seven wave forms (P1–P7) were recorded for each. Middle latency potentials were recorded in response to two decibel levels (65 & 70 dB) and latencies and amplitudes of the four wave forms (Po, Na, Pa, and N2) were recorded for each. The effect of 70 dB is shown for illustrative purposes. We observed no significant effects of genotype, sex, or interactions involving genotype for any measure of AEP response (Supplementary Figure S6). All mice responded in the normal range, indicating that auditory stimuli were being processed. These results suggest that *Upf3b*-null mice have no deficit in auditory sensitivity or processing. Thus, the PPI and startle reflex magnitude deficits in *Upf3b*-null mice are independent of an auditory defect.

Upf3b-null neurons have reduced mature dendritic spines

Previous studies have demonstrated that several mouse models with perturbed neural function defects have dendritic spine defects[43,48,49,50]. To examine whether *Upf3b*-null mice harbor dendritic spine defects, we examined dendritic spine density and morphology using Golgi staining and bright-field confocal microscopy (Figure 3a). In cortical pyramidal neurons, we observed a statistically significant reduction in dendritic spine density in *Upf3b*-null mice relative to control mice (Figures 3a & 3b). We also detected a significant decrease in the dendritic spine density in dentate granule cells of the hippocampus (Figure 3c). As

evidence of specificity, pyramidal neurons in the hippocampal CA1 region did not have significantly reduced dendritic spine density (Figure 3d). To examine the underlying defect, we quantified the different categories of dendritic spines in cortical pyramidal neurons. We found that *Upf3b*-null mice had significantly fewer mature spines than in control mice, but normal numbers of immature spines (Figure 3e). This is consistent with the possibility that UPF3B promotes the maturation of dendritic spines in cortical pyramidal neurons.

Upf3b-null neural progenitors exhibit hyper self-renewal and poorly differentiate

In addition to functioning in neural maturation, we considered the possibility that *Upf3b* has roles in neural development. To test this hypothesis, we performed *in vitro* differentiation assays on cortical mouse neural stem cells (mNSCs) isolated from embryonic *Upf3b*-null and control brains. This revealed several lines of evidence that *Upf3b*-null mNSCs have a defect in their capacity to differentiate. First, *Upf3b*-null mNSCs grown under multipotent differentiating conditions for five days had lower expression of several early neuronal marker genes (*Tuj1 [Tubb3], NeuroD1,* and *Psd95*) compared to wild-type mNSCs (Figure 4a). As further evidence of their immature status, *Upf3b*-null mNSC cultures also had reduced expression of *Ascl1* (Figure 4a), which is considered a master transcriptional regulator for neuronal differentiation[51]. Second, NPC marker genes (*Nestin* and *Sox2*) were expressed at higher levels in *Upf3b*-null cells grown under differentiation conditions, as compared to control cells (Figure 4b). Third, immunofluorescence/cell count analysis demonstrated that *Upf3b*-null cultures grown under multipotent differentiation conditions had a greater percentage of cells expressing the NPC marker, SOX2, and a lower percentage of cells expressing the differentiation marker, TUBB3 (Figure 4c and Supplementary Figures S7a & S7b). Fourth, pulse-chase EdU-labeling followed by immunofluorescence analysis showed that the percentage of cells undergoing self-renewing divisions (i.e., giving rise to SOX2-positive progeny[52,53]) was higher for *Upf3b*-null cultures than control cultures (Figure 4d and Supplementary Figure S7b). This higher rate of self-renewal is consistent with a differentiation defect. Lastly, pulse-chase EdU-labeling followed by immunofluorescence analysis with the proliferation marker, KI-67, demonstrated that *Upf3b*-null cultures were more proliferative than control cultures (Figure 4e and Supplementary Figure S7c). Together, these results indicated that *Upf3b* normally serves to limit mNSC self-renewal and to promote neurogenesis.

To further assess the role of *Upf3b* in neuronal differentiation and maturation, we cultured *Upf3b*-null and control mNSCs under conditions that preferentially drive the differentiation and maturation of neurons (as opposed to glial cells; see Materials and Methods). Over an extended culture period, we assayed their ability to undergo electrical firing. A multi-electrode array system was used to examine spontaneous firing and synchronized spontaneous firing. During our 4-week analysis, we observed a dramatic delay in the synchronized spontaneous firing in *Upf3b*-null cells as compared to wild-type cells (Figure 4f). The firing pattern of *Upf3b*-null and control cells only become comparable after 4 weeks *in vitro* culture (Figure 4f). However, even after 4-weeks culture, the frequency of spontaneous electrical activity was significantly less in *Upf3b*-null cells compared to control cells (Figure 4g). We conclude that neural cells differentiated from *Upf3b*-null nNSCs have a profound defect in spontaneous electrical firing.

Identification *Upf3b*-regulated transcripts in the frontal cortex

Given that UPF3B is a critical factor in a degradation pathway that has roles in neural development and function, we elected to identify transcripts regulated by UPF3B in a neural context *in vivo*. To this end, we performed RNA-seq analysis on frontal cortices from *Upf3b*-null and control mice. Principal components analysis (PCA) demonstrated that the transcriptome signatures of *Upf3b*-null and control frontal cortices from individual mice clustered separately (Figure 5a). A total of 141 genes were significantly upregulated in the *Upf3b*-null samples as compared to control samples ($q < 0.05$; >1.41-fold change) (Figure 5b; Supplementary Table 1). Since NMD is a RNA degradation pathway, these genes upregulated by loss of UPF3B are candidates to transcribe NMD direct target RNAs. In contrast, only 23 genes were downregulated in *Upf3b*-null mice cortices as compared to control cortices (Figure 5b; Supplementary Table 1). The finding that ~5-fold more RNAs were significantly upregulated mRNAs than downregulated is consistent with the possibility that most of the upregulated mRNAs are NMD direct targets. Another possibility is that *Upf3b* negatively regulates many transcripts through an indirect mechanism. Gene ontology analysis[38] of the upregulated genes revealed enrichment for numerous functional categories, including several functions related to “Adhesion” (Figure 5c). Some genes in these groups overlapped with those in the “Behavior” category and have known roles in neural-specific functions, as described in the Discussion. To examine whether any of these putative mouse NMD target mRNAs are conserved in humans, it would be optimal to compare with human frontal cortex or at least human neural-derived cells, but NMD-regulated transcripts have not been identified in such contexts. Thus, we instead compared with human genes shown to be regulated by NMD in human embryonic stem cells (upregulated in response to depletion of UPF1[54] and identified 10 genes in common with those upregulated in *Upf3b*-null mouse frontal cortex (*AGO4, CDH24, ERCC8, FBN2, HIVEP3, RMST, MOV10, PVT1, TNC*, and *WDR83*). Given that different types of cells were compared, we regard this as an underestimate of conserved NMD targets.

As described in the Introduction, the most reliable feature that targets RNAs for degradation by the NMD pathway is an exon-exon junction >55 nt downstream of the stop codon defining the end of the main ORF (“dEJ”). We found that 17% of genes upregulated in *Upf3b*-null frontal cortex (45 of 264) had at least one transcript isoform with a dEJ (Supplementary Table 2). In contrast, only 6% of the downregulated genes (2 of 34) encoded known RNA isoforms with a dEJ (Supplementary Table 2). The presence of a dEJ was statistically enriched for upregulated transcripts as compared to downregulated and unchanged transcripts ($p < 0.0005$) (Figure 5d). We also examined two other features—long 3′ UTRs and upstream (u) ORFs[55]—both of which are known to inconsistently trigger NMD, and found that neither of these features were enriched in transcripts upregulated in *Upf3b*-null frontal cortex (Supplementary Table 2).

DISCUSSION

A growing body of literature supports the notion that NMD factors are critical for both developing and mature neurons in a wide range of organisms. For example, in *D. melanogaster*, loss of NMD factors leads to defects in synapse architecture and reduction

in neurotransmitter strength[56]. Similar phenotypic defects are caused by mutations in any of several different NMD factor genes (*smg1, upf2,* or *smg6)*, suggesting that perturbed NMD (and not another function) is responsible for these fly neural defects. Likewise, in zebrafish embryos, depletion of any of a number of NMD factors (Upf1, Upf2, Smg5, Smg6, or Smg7) causes similar brain development abnormalities, including severe patterning defects[57]. In mice, global loss of most NMD factors leads to early embryonic lethality, precluding analysis of their role in brain development[19,58–61]. To specifically examine the role of NMD in mouse neurons, the NMD factor gene, *Upf2*, was conditionally mutated using Cre-loxP technology, leading to defects in both neural synaptic maturation and axon guidance[62,63]. Mice haploinsufficient for any of a number of EJC factor genes (*Magoh, Rbm8a*, or *Eif4a3*) suffer from microcephaly accompanied by premature neural differentiation and apoptosis[64,65]. Deficiencies in EJC factors also appears to cause neural disease in humans. For example, deletions in 1q21.1, a small region of human chromosome 1 that includes the gene encoding the EJC core component, RBM8A, has been found to be associated with increased incidence of ID, epilepsy, ASD, and SCZ[66]. Indeed, copy number alterations in several EJC and NMD factor genes (*RBM8A, EIF4A3*, *UPF3A, SMG6,* and *RNPS1*) are significantly enriched in patients with neurodevelopmental disorders[67].

In this paper, we focus on *UPF3B*, the only NMD gene that has been definitively shown to have a role in cognition in humans. In particular, mutations in *UPF3B* have been shown—through pedigree analysis—to cause mild-to-severe ID[20,23–29,31,68,69]. Many patients with *UPF3B* mutation also suffer from neurodevelopmental disorders, including SCZ, ADHD, and ASD, providing evidence that *UPF3B*, and by implication, NMD, have roles in developmental processes required for normal behavior. To understand the underlying basis for these defects, we generated a mouse model with a null mutation in the *Upf3b* gene. These NMD-deficient mice exhibit specific impairments in fear-conditioned memory and sensorimotor gating (Figures 1 & 2) that we postulate stem from the neurogenesis and neuronal maturation defects that we defined in cultured *Upf3b*-null mNSCs (Figure 4 and Supplementary Figure S7). Another factor potentially contributing to the behavioral defects of *Upf3b*-null mice is reduced dendritic spine density that we showed occurs in specific neuronal populations (Figure 3). To define the RNAs misregulated as a result of NMD deficiency, we performed transcriptome profiling on *Upf3b*-null and control frontal cortices. Among the misregulated RNAs were many high-confidence direct NMD target mRNAs encoding proteins known to be critical for neural processes.

Behavioral deficits in *Upf3b*-null mice

Our behavioral analysis revealed that *Upf3b*-null mice were normal in spatial memory tasks (Supplementary Figure S4), but exhibited both contextual and cued conditional fear-learning defects (Figures 1a & 1b). By analogy, neuroligin-3 (*Nlgn3*)-null mice, a model of ASD, also exhibit both of these fear-based defects but are normal in spatial memory[70]. NLGN3 is a cell-surface protein expressed on neurons involved in CNS synapse formation and remodeling[71]. We suggest NMD may control the same events through its ability to degrade mRNAs encoding synapse formation and remodeling proteins. The amygdala, hippocampus, and the prefrontal cortex are all critical for fear memory recognition and downstream processes[72–74], including storing fear memories[72]. It will be intriguing in the

future to delineate which specific brain regions and neural circuits require UPF3B for fear-conditioned learning.

Upf3b-null mice also have a striking deficit in PPI, a measure of sensorimotor gating (Figures 2c–f). PPI deficits have been reported in a variety of human neuropsychiatric disorders, including SCZ, as well as mouse models displaying ID and ASD, such as *Fmr1*-, *Fmr1/Fxr2-, Nrxn1a-,* and *Pten*-KO mice[75–78]. Interestingly, several mouse mutants (including *Fmr1*-KO mice) also harbor deficits in the magnitude of the acoustic startle reflex[75], just as we found for *Upf3b*-null mice (Figure 2a & 2b). Future studies will be directed towards determining the underlying mechanism responsible for the PPI deficits in *Upf3b*-null mice. Reduced PPI can result from perturbations of normal activity within distributed neural circuitry connecting several different brain regions, including the prefrontal- and limbic-cortical, striatal, pallidal, thalamic and pontine structures[47]. Our finding that the PPI deficit in *Upf3b*-null mice is not significantly "rescued" by haloperidol (Figure S5) suggests that it does not reflect subcortical (striatal or n. accumbens) dopamine hyperfunction[47]. PPI deficits in schizophrenia patients are also not rescued by treatment with haloperidol[79].

Both PPI and fear-conditioned learning are regulated by the prefrontal cortex[43] and thus the abnormally low dendritic spine density we observed in *Upf3b*-null prefrontal cortex pyramidal neurons (Figure 3) may contribute to one or both of these behavioral defects. Consistent with this, reduced cortical dendritic spine density is an often-reported neural deficits in SCZ and ID patients, as well as mouse models for these conditions[80–83]. It will be intriguing in the future to determine whether a common defect underlies the learning/memory and PPI deficits in *Upf3b*-null mice.

We found that *Upf3b*-null mice have a selective reduction in mature, not immature, dendritic spines (Figure 3e), suggesting that NMD promotes dendritic spine maturation. NMD may do this through regulation of mRNAs encoding proteins involved in this process. Alternatively, this regulation may occur locally—such as in the dendrites themselves—as UPF3B has been previously identified in dendrites and dendritic spines of mouse primary E17.5 hippocampal neurons, using tagged recombinant UPF3B protein[26]. Other NMD factors—UPF1, UPF2, and SMG1—have been shown to be enriched in axons of distal commissural axons in the developing mouse spinal cord[62]. NMD is a regulated process in developing neurons[28,29], and thus we suggest that this pathway may selectively degrade transcripts in dendrites in a developmentally regulated manner in order to influence their maturation. While we do not know the physiological consequences of the dendritic spine defect in *Upf3b*-null mice, it is tempting to speculate that it has a role in one or more of the behavioral defects in these mice. This follows from the roles of dendritic spines in synaptic connectivity and the fact that mice with many different types of behavioral defects also have deficient dendritic spines. Relevant to our study, PPI-deficient mouse models have been shown to exhibit abnormal cortical and hippocampal dendritic spine morphology[43,48] and mice harboring fear conditioning and sleep defects exhibit remodeled dendritic spines in the cortex[49,50].

The role of *Upf3b* in neurogenesis

To investigate whether *Upf3b*-null mice have neurogenesis defects that could be responsible for their behavioral defects, we generated and analyzed mNSC lines from *Upf3b*-null and control embryos. We found that *Upf3b*-null mNSCs exhibit increased self-renewal and decreased neurogenesis relative to control mNSCs (Figure 4 and Supplementary Figure S7), suggesting that UPF3B serves to promote NSC differentiation. A similar conclusion was reached by Jolly *et al.*, who found that depletion of UPF3B (by RNAi) from later stage neurons (E18.5 NSCs and isolated hippocampal neurons) inhibited their differentiation or maturation[31]. We also found that the development of electrical activity is impaired in *Upf3b*-null NSC-derived neurons (Figures 4f & 4g, Supplementary Figure S7d). This raises the possibility that UPF3B promotes not only early neurogenesis but also neuronal maturation. However, it is also possible that the electrical firing defect results from inefficient differentiation at an earlier stage of neural development (Figure 4 and Supplementary Figure S7). While a differentiation defect may be a contributing factor, several lines of evidence suggest that a maturation defect also has a role in the impaired electrical activity of *Upf3b*-null neural cells. First, we used culture condition known to efficiently generate neurons for our electrophysiology experiments[30]. Second, *Upf3b*-null NSCs began differentiating very soon after being put under such culture conditions (~35% began differentiating, based on two markers, after only 3 days of culture [Fig 4c]), yet these *Upf3b*-null do not generate significant action potentials until much later (after 28 days in culture, with little or no activity after 7, 14, or 21 days in culture [Fig 4g]). Third, we previously reported that mouse NSCs depleted of UPF3B (using RNAi) undergo less than one additional division (on average) before differentiation, making it unlikely that UPF3B depletion simply lead to an accumulation of undifferentiated proliferating cells[31]. Finally, our finding that *Upf3b*-null mice have dendritic spine defects (Figure 3) is supportive of a role in UPF3B in neural maturation *in vivo*. Regardless of the precise roles of UPF3B in neural differentiation and maturation, our analysis clearly indicates that UPF3B is critical for the efficient and timely generation of functional neurons *in vitro*, providing an explanation for the behavioral defects caused by loss of functional UPF3B *in vivo*.

Accumulating data suggest that UPF3B is highly regulated during neuronal development. For instance, both *UPF3B* mRNA and UPF3B protein were shown to be downregulated in a rat neural stem line upon differentiation[84]. In contrast, *Upf3b* mRNA expression increases during cortical neuron maturation, with highest level in synaptically active neuronal networks[31]. Consistent with this upregulated pattern of expression, *Upf3b* is expressed at higher level in adult brains than embryonic and postnatal mice brains *in vivo*[31]. Interestingly, *Upf3b* expression in mature neurons is also regulated by synaptic activity; depolarization of hippocampal neuron depresses Upf3b expression[31]. Spatially, both *Upf3b* mRNA and UPF3B protein are broadly expressed in most structures and cell types in the brain, but they are differentially expressed in some specific brain regions. While the function of UPF3B in mature neurons is not known, it is present in not only in the cell body, but also neurites[31,84], consistent with evidence that NMD regulates synaptic transmission and targets mRNAs that function at the synapse in mammalian cells[85,86]. In flies, even hemizygous mutations in NMD factor genes have been shown to be sufficient to disturb synapse structure and function[56]. NMD also functions in axon guidance, as shown in mouse commissural

neurons[87]. In the future, it will be important to define the specific roles of UPF3B at the synapse, in axon guidance, and other functions in mature neurons.

Our findings that UPF3B promotes neural differentiation is in apparent contradiction with our laboratory's previous finding that another NMD factor, UPF1, inhibits neural differentiation[28]. In that study, we found that depletion of UPF1 was sufficient to trigger multi-potent P19 cells to differentiate down the neural cell lineage[28]. Conversely, preventing the UPF1 downregulatory response that is normally triggered by neural differentiation cues largely prevented neural differentiation of both P19 and mNSCs, as judged by both neural and stem cell markers. How does one reconcile these results in light of the findings reported here? One possibility is that NMD has opposite effects on different stages of neural development. Thus, while NMD promotes the proliferative and stem-like state of multipotent cells [represented by P19 cells[88]], it may instead promote the differentiation of already committed neural stem cells (represented by mNSCs). In support of this, we previously found that while depletion of UPF1 in mNSCs decreased the level of pluripotency markers (such as *Oct4* and *Nanog*), it *increased* neural stem markers, such as *Sox2, Nestin,* and *Dcx*[28]. This is analogous to what we observed in response to loss of UPF3B (Fig. 4).

A non-mutually exclusive possibility is that UPF1 and UPF3B have different functions. Because UPF3B appears to drive a specific branch of the NMD pathway[16,89], it may promote the decay of a specific subset of transcripts that promotes neural differentiation. In contrast, because UPF1 is an essential NMD factor that appears to be required for all NMD branches[16,18], it may degrade a larger set of transcripts that, on balance, promote the opposite response – maintenance of the stem-like state. While the UPF3B-dependent branch of NMD may exhibit unique effects in neural cells, it is worthy of note that in another system—human embryonic stem cells—UPF1 and UPF3B manipulation (whether depletion or forced expression) have very similar effects on primary germ layer differentiation[90].

The neural defects caused by loss of *Upf3b* are strikingly different from the phenotypic consequences of loss-of-function mutations in other NMD genes. Mutational inactivation of *Upf1, Upf2, Upf3a, Smg1*, or *Smg6* leads to early embryonically lethality, at the pre- or peri-implantation stage[19,58–61]. One explanation for why loss of *Upf3b* does not cause embryonic lethality is because it encodes a NMD branch-specific factor[16,21]. By promoting the decay of only a subset of NMD substrates, UPF3B might only drive specific developmental events *in vivo*, such as those involving brain development, but not those involving early embryonic development. Another possibility is that UPF3B is a NMD amplifier and thus developing cells that either require high levels of NMD and/or are particularly sensitive to alterations in NMD magnitude will be specifically perturbed by loss of UPF3B.

Upf3b-regulated transcripts in the cerebral cortex

To begin to understand the molecular roles of UPF3B in the nervous system, we performed transcriptome profiling of *Upf3b*-null vs. control frontal cortex. A remarkably specific cohort of mRNAs were upregulated and thus candidates to be degraded by the NMD pathway. Table 1 lists *Upf3b*-regulated genes that have been shown to have functions in the

nervous system and neural disease. Intriguingly, 20 of the 21 coding genes have at least one NMD-inducing features, suggesting many of them encode direct NMD target RNAs. Several of these encode adhesion proteins involved in neural processes, including DSCAM, DSCAML1, PCDH15, ITGA8, SDK2, and CDH24. DSCAM and its paralog, DSCAML1, are transmembrane proteins critical for cortical neural networks; they perform a variety of functions, including dendritic self-avoidance, dendritic arborization, and promotion of axon growth and synaptic connections. The integrin, ITGA8, and the cadherin protein, CDH24, are both involved in synaptic adhesion through promoting neurite and/or axonal outgrowth. *CDH24* mRNA appears to be a conserved target of NMD, as it was also identified as being degraded by NMD in human ES cells[90]. PCDH15 is another member of the cadherin superfamily; it is broadly expressed in the embryonic brain and is critical for forming filaments in sensory hair cells in the developing inner ear. In addition to targeting mRNAs encoding adhesion proteins directing synaptic connections and activity, UPF3B may also promote the decay of mRNAs encoding the ligands involved in these events. As a case in point, the UPF3B-regulated transcript, *Sema4g*, encodes a member of a large family of secreted proteins, some of which serve as axon guidance ligands.

Interestingly, some UPF3B-targeted transcripts encode proteins involved in retinal neural cell connectivity. For example, DSCAM and DSCAML1 function in dendritic self-avoidance of specific interneuron types, leading to lamina-specific synaptic connections in the mammalian retina. We also identified *Sdk2* and *Col18a1* as UPF3B-regulated mRNAs. The former encodes a member of the immunoglobulin superfamily that promotes lamina-specific synaptic connections in the retina and is specifically required for the formation of neuronal circuits that detect motion. The latter encodes a type XVIII collagen deposited in the extracellular matrix that is thought to have roles in retina formation. These putative NMD targets involved in eye development are of interest, as increasing evidence suggests roles for NMD in the eye. For example, in *D. melanogaster*, genetic mosaic analysis revealed that cell clones lacking functional *Upf1* or *Upf2* fail to contribute to the eye in adult flies[91]. If wild-type cells are eliminated from these mosaic animals, the remaining NMD-deficient cells proliferate and differentiate to form eyes but they are smaller than normal and disorganized. This suggests that NMD acts by promoting the proliferation and patterning of neural cells that form the insect eye. In humans, the loss of the entire NMD pathway is likely to be embryonic lethal (based on mouse knockout studies[19,58–61]) and thus a direct comparison with these fly studies cannot be made, but it is known that many patients with mutations in the NMD branch-specific factor gene, *UPF3B*, suffer from strabismus and/or cataracts[26].

Other UPF3B-regulated transcripts of potential relevance to the nervous system are *Fbn2, Tnc, Kcnh4, Ptch1, Rmst,* and *Brca2. Fbn2* and *Tnc* both encode extracellular matrix proteins and thus represent putative NMD targets in the same general class as those encoding adhesion proteins, as described above. *Fbn2* encodes FIBRILIN-2, a component of connective tissue microfibrils that is critical for TGF-β bioavailability[92], and thus it may have a role in the known ability of NMD to regulate TGF-β signaling events critical for neurogenesis and other developmental pathways[28,90]. *Tnc* encodes tenascin C, a glycoprotein that is restricted in its expression in the CNS to neurogeneic areas. Both *Tnc* and *Fbn2* mRNA appears to be a conserved NMD targets, based on them being upregulated not only in mouse *Upf3b*-null cortex (herein), but NMD-deficient human cells[16,90]. *Kcnh4*

encodes a potassium voltage-gated channel expressed in both the neocortex and the striatum and thus is likely to be involved in cellular excitability in neurons in these regions of the CNS. *Ptch1, Rmst,* and *Brca2* are all critical for neurogenesis. *Ptch1* encodes a receptor for the secreted signaling molecule, sonic hedgehog, which has important roles in various aspects of neural development, including motor neuron generation and neurogenesis in the adult hippocampus. *Rmst* is a non-coding RNA that cooperates with SOX2 to influence neural stem cell fate and neuronal differentiation[93]. While non-coding RNAs are seemingly paradoxical NMD targets given that NMD requires translation[94], it has recently come to light that even though non-coding RNAs do not encode large proteins, many of them are translated, based on polysome and genome-wide ribosome profiling analysis[95–99]. *Brca2* encodes a multifunctional DNA-binding protein critical for repair of DNA strand breaks. While best known as a tumor suppressor gene in epithelial cells, BRCA2 is also critical for neurons, as it repairs DNA-strand breaks that occur naturally during neurogenesis[100]. Indeed, many neurally expressed genes and their promoters undergo DNA breakage at relatively high frequency[101,102] and thus the possibility that NMD influences repair of these breaks through regulated decay of *BRCA2* mRNA is of considerable interest.

The human orthologs corresponding to several mouse UPF3B-regulated genes are implicated in human neural diseases. For example, many UPF3B KO-upregulated candidate NMD target mRNAs that we identified in *Upf3b*-null cerebral cortex correspond to recently defined SCZ disease risk genes (*DSCAM, HIVEP3, MOV10, NIN, SPEN, AKR1C2, ARL5C, CD59,* and *VWA5B1*)[103]. Among these disease risk genes is *DSCAM*, which encodes Down syndrome cell adhesion molecule, a transmembrane protein that is highly expressed in the developing fetal CNS. It is encoded by chromosome 21 in humans and causes Down syndrome symptoms when overexpressed. Another UPF3B-regulated gene is *Pcdh15*, which when mutated in humans causes Usher Syndrome type 1F, a developmental disorder that presents with visual, hearing, and sleep defects, and, in some cases, neuropsychiatric symptoms, including ASD and biopolar disorder. Finally, mutations in the UPF3B-regulated gene, *Col18a1,* cause one form of Knobloch syndrome, which presents with severe eyesight problems, cataracts, and retinal degeneration.

In summary, our study introduces a mouse model that has the potential to elucidate the *in vivo* roles of a highly conserved and selective RNA decay pathway in neuronal development and behavior. Intriguingly, these *Upf3b*-null mice exhibit strikingly similar phenotypes as mouse models for other human neurodevelopmental disorders. This raises the possibility that the steady-state levels of specific mRNAs encoding proteins important for pathways critical for normal neural development are regulated by NMD. Given that *Upf3b*-null mice exhibit behavioral defects that mimic, in some respects, those of humans with *UPF3B* mutations, these mice may also serve as a model system to understand the neuropathology in these patients. Not only may this reveal the underlying basis for their learning and memory deficits, but the PPI deficits in *Upf3b*-null mice may prove useful in understanding the basis for impaired PPI in a wide variety of human brain disorders, including SCZ. Our identification of dysregulated transcripts in the cerebral cortex of these NMD-deficient mice provides an important resource for future investigations into the molecular basis for behavioral defects, including those impinging on normal learning and sensorimotor gating.

We suggest that the study of NMD provides a novel portal into key genes critical for normal neural development and behavior.

Supplementary Material

Refer to Web version on PubMed Central for supplementary material.

Acknowledgments

This research was supported by National Institutes of Health grants GM111838 (MFW), MH59803 (NRS), MH94320 (NRS), T32 EB00938008 (SJ), as well as a Howard Hughes Medical Institute international fellow award (ES), a Distinguished Investigator Award from the Brain & Behavior Research Foundation (NRS), and a National Health & Medical Research Council grant APP1063808 (JG, MFW, and LJ), the Australian Research Council Discovery Early Career Research Award DE160100620 (LJ). We are grateful to Dr. Martin Marsala (UCSD) and Marián Hruška-Plocháň (UCSD) for helping with mNSC isolation, mNSC differentiation, and electrophysiology recordings. We also thank Kristin Jepsen and the IGM Genomics Center, University of California, San Diego, La Jolla, CA, for performing RNAseq analyses.

References

1. Chang Y-F, Imam JS, Wilkinson MF. The nonsense-mediated decay RNA surveillance pathway. Annu Rev Biochem. 2007; 76: 51–74. [PubMed: 17352659]
2. He F, Li X, Spatrick P, Casillo R, Dong S, Jacobson A. Genome-Wide Analysis of mRNAs Regulated by the Nonsense-Mediated and 5′ to 3′ mRNA Decay Pathways in Yeast. Mol Cell. 2003; 12: 1439–1452. [PubMed: 14690598]
3. Huang L, Wilkinson MF. Regulation of nonsense-mediated mRNA decay. Wiley Interdiscip Rev RNA. 2012; 3: 807–828. [PubMed: 23027648]
4. Mendell JT, Sharifi NA, Meyers JL, Martinez-Murillo F, Dietz HC. Nonsense surveillance regulates expression of diverse classes of mammalian transcripts and mutes genomic noise. Nat Genet. 2004; 36: 1073–8. [PubMed: 15448691]
5. Ramani AK, Nelson AC, Kapranov P, Bell I, Gingeras TR, Fraser AG. High resolution transcriptome maps for wild-type and nonsense-mediated decay-defective Caenorhabditis elegans. Genome Biol. 2009; 10: R101. [PubMed: 19778439]
6. Wittmann J, Hol EM, Jäck H-M. hUPF2 silencing identifies physiologic substrates of mammalian nonsense-mediated mRNA decay. Mol Cell Biol. 2006; 26: 1272–87. [PubMed: 16449641]
7. Nicholson P, Yepiskoposyan H, Metze S, Zamudio Orozco R, Kleinschmidt N, Mühlemann O, et al. Nonsense-mediated mRNA decay in human cells: mechanistic insights, functions beyond quality control and the double-life of NMD factors. Cell Mol life Sci. 2010; 67: 677–700. [PubMed: 19859661]
8. Karam R, Wengrod J, Gardner LB, Wilkinson MF. Regulation of nonsense-mediated mRNA decay: implications for physiology and disease. Biochim Biophys Acta. 2013; 1829: 624–33. [PubMed: 23500037]
9. Smith JE, Baker KE. Nonsense-mediated RNA decay - a switch and dial for regulating gene expression. BioEssays. 2015; 37: 612–623. [PubMed: 25820233]
10. Fatscher T, Boehm V, Gehring NH. Mechanism, factors, and physiological role of nonsense-mediated mRNA decay. Cell Mol Life Sci. 2015; 72: 4523–4544. [PubMed: 26283621]
11. Lykke-Andersen S, Jensen TH. Nonsense-mediated mRNA decay: an intricate machinery that shapes transcriptomes. Nat Rev Mol Cell Biol. 2015; 16: 665–677. [PubMed: 26397022]
12. Nagy E, Maquat LE. A rule for termination-codon position within intron-containing genes: when nonsense affects RNA abundance. Trends Biochem Sci. 1998; 23: 198–9. [PubMed: 9644970]
13. Boehm V, Gehring NH. Exon Junction Complexes: Supervising the Gene Expression Assembly Line. Trends Genet. 2016; 32: 724–735. [PubMed: 27667727]
14. Rebbapragada I, Lykke-Andersen J. Execution of nonsense-mediated mRNA decay: what defines a substrate? Curr. Opin Cell Biol. 2009; 21: 394–402.

15. Barrett LW, Fletcher S, Wilton SD. Regulation of eukaryotic gene expression by the untranslated gene regions and other non-coding elements. Cell Mol life Sci. 2012; 69: 3613–34. [PubMed: 22538991]
16. Chan WK, Huang L, Gudikote JP, Chang YF, Imam JS, MacLean JA 2nd, et al. An alternative branch of the nonsense-mediated decay pathway. EMBO J. 2007; 26: 1820–1830. [PubMed: 17363904]
17. Metze S, Herzog VA, Ruepp M-D, Mühlemann O. Comparison of EJC-enhanced and EJC-independent NMD in human cells reveals two partially redundant degradation pathways. RNA. 2013; 19: 1432–48. [PubMed: 23962664]
18. Gehring NH, Neu-Yilik G, Breit S, Viegas MH, Hentze MW, et al. Exon-junction complex components specify distinct routes of nonsense-mediated mRNA decay with differential cofactor requirements. Mol Cell. 2005; 20: 65–75. [PubMed: 16209946]
19. Weischenfeldt J, Damgaard I, Bryder D, Theilgaard-Monch K, Thoren LA, Nielsen FC, et al. NMD is essential for hematopoietic stem and progenitor cells and for eliminating by-products of programmed DNA rearrangements. Genes Dev. 2008; 22: 1381–1396. [PubMed: 18483223]
20. Tarpey PS, Raymond FL, Nguyen LS, Rodriguez J, Hackett A, Vandeleur L, et al. Mutations in UPF3B, a member of the nonsense-mediated mRNA decay complex, cause syndromic and nonsyndromic mental retardation. Nat Genet. 2007; 39: 1127–33. [PubMed: 17704778]
21. Huang L, Lou C-HH, Chan W, Shum EY, Shao A, Stone E, et al. RNA homeostasis governed by cell type-specific and branched feedback loops acting on NMD. Mol Cell. 2011; 43: 950–61. [PubMed: 21925383]
22. Karam R, Lou C-H, Kroeger H, Huang L, Lin JH, Wilkinson MF. The unfolded protein response is shaped by the NMD pathway. EMBO Rep. 2015.
23. Lynch SA, Nguyen LS, Ng LY, Waldron M, McDonald D, Gecz J. Broadening the phenotype associated with mutations in UPF3B: two further cases with renal dysplasia and variable developmental delay. Eur J Med Genet. 55: 476–9. [PubMed: 22609145]
24. Xu X, Zhang L, Tong P, Xun G, Su W, Xiong Z, et al. Exome sequencing identifies UPF3B as the causative gene for a Chinese non-syndrome mental retardation pedigree. Clin Genet. 2013; 83: 560–4. [PubMed: 22957832]
25. Addington AM, Gauthier J, Piton A, Hamdan FF, Raymond A, Gogtay N, et al. A novel frameshift mutation in UPF3B identified in brothers affected with childhood onset schizophrenia and autism spectrum disorders. Mol Psychiatry. 2011; 16: 238–239. [PubMed: 20479756]
26. Laumonnier F, Shoubridge C, Antar C, Nguyen LS, Van Esch H, Kleefstra T, et al. Mutations of the UPF3B gene, which encodes a protein widely expressed in neurons, are associated with nonspecific mental retardation with or without autism. Mol Psychiatry. 2010; 15: 767–776. [PubMed: 19238151]
27. Szyszka P, Sharp SI, Dedman A, Gurling HMD, McQuillin A. A nonconservative amino acid change in the UPF3B gene in a patient with schizophrenia. Psychiatr Genet. 2012; 22: 150–151. [PubMed: 21862950]
28. Lou CH, Shao A, Shum EY, Espinoza JL, Huang L, Karam R, et al. Posttranscriptional control of the stem cell and neurogenic programs by the nonsense-mediated RNA decay pathway. Cell Rep. 2014; 6: 748–64. [PubMed: 24529710]
29. Bruno IG, Karam R, Huang L, Bhardwaj A, Lou CH, Shum EY, et al. Identification of a microRNA that activates gene expression by repressing nonsense-mediated RNA decay. Mol Cell. 2011; 42: 500–10. [PubMed: 21596314]
30. Yuan SH, Martin J, Elia J, Flippin J, Paramban RI, Hefferan MP, et al. Cell-surface marker signatures for the Isolation of neural stem cells, glia and neurons derived from human pluripotent stem cells. PLoS One. 2011; 6. doi: 10.1371/journal.pone.0017540.
31. Jolly LA, Homan CC, Jacob R, Barry S, Gecz J. The UPF3B gene, implicated in intellectual disability, autism, ADHD and childhood onset schizophrenia regulates neural progenitor cell behaviour and neuronal outgrowth. Hum Mol Genet. 2013; 22: 4673–87. [PubMed: 23821644]
32. Barros CS, Calabrese B, Chamero P, Roberts AJ, Korzus E, Lloyd K, et al. Impaired maturation of dendritic spines without disorganization of cortical cell layers in mice lacking NRG1/ErbB

signaling in the central nervous system. Proc Natl Acad Sci U S A. 2009; 106: 4507–12. [PubMed: 19240213]

33. Roberts AJ, Krucker T, Levy CL, Slanina KA, Sutcliffe JG, Hedlund PB. Mice lacking 5-HT receptors show specific impairments in contextual learning. Eur J Neurosci. 2004; 19: 1913–22. [PubMed: 15078565]
34. Li H, Radford JC, Ragusa MJ, Shea KL, McKercher SR, Zaremba JD, et al. Transcription factor MEF2C influences neural stem/progenitor cell differentiation and maturation in vivo. Proc Natl Acad Sci U S A. 2008; 105: 9397–402. [PubMed: 18599437]
35. Dobin A, Gingeras TR. Mapping RNA-seq Reads with STAR. Curr Protoc Bioinformatics. 2015; 51: 11.14.1–11.14.19. [PubMed: 26334920]
36. Dobin A, Davis CA, Schlesinger F, Drenkow J, Zaleski C, Jha S, et al. STAR: ultrafast universal RNA-seq aligner. Bioinformatics. 2013; 29: 15–21. [PubMed: 23104886]
37. Ramsköld D, Wang ET, Burge CB, Sandberg R. An abundance of ubiquitously expressed genes revealed by tissue transcriptome sequence data. PLoS Comput Biol. 2009; 5: e1000598. [PubMed: 20011106]
38. Sherman BT, Huang DW, Tan Q, Guo Y, Bour S, Liu D, et al. DAVID Knowledgebase: a gene-centered database integrating heterogeneous gene annotation resources to facilitate high-throughput gene functional analysis. BMC Bioinformatics. 2007; 8: 426. [PubMed: 17980028]
39. Huang DW, Sherman BT, Lempicki RA. Systematic and integrative analysis of large gene lists using DAVID bioinformatics resources. Nat Protoc. 2009; 4: 44–57. [PubMed: 19131956]
40. Shum EY, Espinoza JL, Ramaiah M, Wilkinson MF. Identification of novel post-transcriptional features in olfactory receptor family mRNAs. Nucleic Acids Res. 2015. gkv324.
41. Belzung C, Le Pape G. Comparison of different behavioral test situations used in psychopharmacology for measurement of anxiety. Physiol Behav. 1994.
42. Lalonde R, Strazielle C. Brain regions and genes affecting limb-clasping responses. Brain Res Rev. 2011.
43. Swerdlow N, Weber M, Qu Y, Light G, Braff D. Realistic expectations of prepulse inhibition in translational models for schizophrenia research. Psychopharmacology (Berl). 2008.
44. Braff D, Geyer M, Swerdlow N. Human studies of prepulse inhibition of startle: normal subjects, patient groups, and pharmacological studies. Psychopharmacology (Berl). 2001.
45. Braff D, Stone C, Callaway E, Geyer M, Glick I, Bali L. Prestimulus effects on human startle reflex in normals and schizophrenics. Psychophysiology. 1978; 15: 339–43. [PubMed: 693742]
46. Swerdlow NR, Braff DL, Geyer MA. Sensorimotor gating of the startle reflex: what we said 25 years ago, what has happened since then, and what comes next. J Psychopharmacol. 2016; 30: 1072–1081. [PubMed: 27539931]
47. Swerdlow NR, Geyer MA, Braff DL. Neural circuit regulation of prepulse inhibition of startle in the rat: current knowledge and future challenges. Psychopharmacology (Berl). 2001; 156: 194–215. [PubMed: 11549223]
48. Geyer M, Mcllwain K, Paylor R. Mouse genetic models for prepulse inhibition: an early review. Mol Psychiatry. 2002.
49. Yang G, Lai CSW, Cichon J, Ma L, Li W, Gan W-B. Sleep promotes branch-specific formation of dendritic spines after learning. Science (80-). 2014; 344: 1173–8.
50. Lai C, Franke T, Gan W. Opposite effects of fear conditioning and extinction on dendritic spine remodelling. Nature. 2012.
51. Raposo AASF, Vasconcelos FF, Drechsel D, Marie C, Johnston C, Dolle D, et al. Ascl1 Coordinately Regulates Gene Expression and the Chromatin Landscape during Neurogenesis. Cell Rep. 2015; 10: 1544–1556. [PubMed: 25753420]
52. Diermeier-Daucher S, Clarke ST, Hill D, Vollmann-Zwerenz A, Bradford JA, Brockhoff G. Cell type specific applicability of 5-ethynyl-2′-deoxyuridine (EdU) for dynamic proliferation assessment in flow cytometry. Cytometry A. 2009; 75: 535–46. [PubMed: 19235202]
53. Limsirichaikul S, Niimi A, Fawcett H, Lehmann A, Yamashita S, Ogi T. A rapid non-radioactive technique for measurement of repair synthesis in primary human fibroblasts by incorporation of ethynyl deoxyuridine (EdU). Nucleic Acids Res. 2009; 37: e31. [PubMed: 19179371]

54. Lou C, Chousal J, Goetz A, Shum E, Brafman D, Liao X, et al. Nonsense-Mediated RNA Decay Influences Human Embryonic Stem Cell Fate. Stem Cell Reports. 2016; 6: 844–857. [PubMed: 27304915]
55. Schweingruber C, Rufener SC, Zünd D, Yamashita A, Mühlemann O. Nonsense-mediated mRNA decay - mechanisms of substrate mRNA recognition and degradation in mammalian cells. Biochim Biophys Acta. 2013; 1829: 612–23. [PubMed: 23435113]
56. Long AA, Mahapatra CT, Woodruff EA, Rohrbough J, Leung H-T, Shino S, et al. The nonsense-mediated decay pathway maintains synapse architecture and synaptic vesicle cycle efficacy. J Cell Sci. 2010; 123: 3303–15. [PubMed: 20826458]
57. Wittkopp N, Huntzinger E, Weiler C, Saulière J, Schmidt S, Sonawane M, et al. Nonsense-mediated mRNA decay effectors are essential for zebrafish embryonic development and survival. Mol Cell Biol. 2009; 29: 3517–28. [PubMed: 19414594]
58. Medghalchi SM, Frischmeyer PA, Mendell JT, Kelly AG, Lawler AM, Dietz HC. Rent1, a trans-effector of nonsense-mediated mRNA decay, is essential for mammalian embryonic viability. Hum Mol Genet. 2001; 10: 99–105. [PubMed: 11152657]
59. McIlwain DR, Pan Q, Reilly PT, Elia AJ, McCracken S, Wakeham AC, et al. Smg1 is required for embryogenesis and regulates diverse genes via alternative splicing coupled to nonsense-mediated mRNA decay. Proc Natl Acad Sci U S A. 2010; 107: 12186–91. [PubMed: 20566848]
60. Li T, Shi Y, Wang P, Guachalla LM, Sun B, Joerss T, et al. Smg6/Est1 licenses embryonic stem cell differentiation via nonsense-mediated mRNA decay. EMBO J. 2015; 34: 1630–1647. [PubMed: 25770585]
61. Shum EY, Jones SH, Shao A, Chousal J, Krause MD, Chan W-K, et al. The Antagonistic Gene Paralogs Upf3a and Upf3b Govern Nonsense-Mediated RNA Decay. Cell. 2016; 165: 382–395. [PubMed: 27040500]
62. Colak D, Ji S-J, Porse BT, Jaffrey SR. Regulation of axon guidance by compartmentalized nonsense-mediated mRNA decay. Cell. 2013; 153: 1252–65. [PubMed: 23746841]
63. Zheng S, Gray EE, Chawla G, Porse BT, O'Dell TJ, Black DL. PSD-95 is post-transcriptionally repressed during early neural development by PTBP1 and PTBP2. Nat Neurosci. 2012; 15: 381–8. S1. [PubMed: 22246437]
64. McMahon JJ, Miller EE, Silver DL. The exon junction complex in neural development and neurodevelopmental disease. Int J Dev Neurosci. 2016; 55: 117–123. [PubMed: 27071691]
65. Mao H, McMahon JJ, Tsai Y-H, Wang Z, Silver DL. Haploinsufficiency for Core Exon Junction Complex Components Disrupts Embryonic Neurogenesis and Causes p53-Mediated Microcephaly. PLOS Genet. 2016; 12: e1006282. [PubMed: 27618312]
66. Nguyen LS, Wilkinson MF, Gecz J. Nonsense-mediated mRNA decay: Inter-individual variability and human disease. Neurosci Biobehav Rev. 2014; 46P2: 175–186.
67. Nguyen LS, Kim H-G, Rosenfeld JA, Shen Y, Gusella JF, Lacassie Y, et al. Contribution of copy number variants involving nonsense-mediated mRNA decay pathway genes to neuro-developmental disorders. Hum Mol Genet. 2013; 22: 1816–25. [PubMed: 23376982]
68. Nguyen LS, Jolly L, Shoubridge C, Chan WK, Huang L, Laumonnier F, et al. Transcriptome profiling of UPF3B/NMD-deficient lymphoblastoid cells from patients with various forms of intellectual disability. Mol Psychiatry. 2012; 17: 1103–15. [PubMed: 22182939]
69. Alachkar A, Jiang D, Harrison M, Zhou Y, Chen G, Mao Y. An EJC factor RBM8a regulates anxiety behaviors. Curr Mol Med. 2013; 13: 887–99. [PubMed: 23638902]
70. Radyushkin K, Hammerschmidt K, Boretius S, Varoqueaux F, El-Kordi A, Ronnenberg A, et al. Neuroligin-3-deficient mice: model of a monogenic heritable form of autism with an olfactory deficit. Genes Brain Behav. 2009; 8: 416–25. [PubMed: 19243448]
71. Philibert RA, Winfield SL, Sandhu HK, Martin BM, Ginns EI. The structure and expression of the human neuroligin-3 gene. Gene. 2000; 246: 303–10. [PubMed: 10767552]
72. Milad MR, Quirk GJ. Neurons in medial prefrontal cortex signal memory for fear extinction. Nature. 2002; 420: 70–4. [PubMed: 12422216]
73. Burgos-Robles A, Vidal-Gonzalez I, Quirk GJ. Sustained conditioned responses in prelimbic prefrontal neurons are correlated with fear expression and extinction failure. J Neurosci. 2009; 29: 8474–82. [PubMed: 19571138]

74. Curzon P, Rustay NR, Browman KE. Chapter 2 Cued and Contextual Fear Conditioning for Rodents. Methods Behav Anal Neurosci. 2014.
75. Nielsen D, Derber W, McClellan D, Crnic L. Alterations in the auditory startle response in< i> Fmr1</i> targeted mutant mouse models of fragile X syndrome. Brain Res. 2002.
76. Kwon C, Luikart B, Powell C, Zhou J. Pten regulates neuronal arborization and social interaction in mice. Neuron. 2006.
77. Spencer C. Exaggerated behavioral phenotypes in Fmr1/Fxr2 double knockout mice reveal a functional genetic interaction between Fragile X-related proteins. Hum Mol Genet. 2006.
78. Rujescu D, Ingason A. Disruption of the neurexin 1 gene is associated with schizophrenia. Hum Mol Genet. 2009.
79. Swerdlow NR, Light GA, Cadenhead KS, Sprock J, Hsieh MH, Braff DL. Startle gating deficits in a large cohort of patients with schizophrenia: relationship to medications, symptoms, neurocognition, and level of function. Arch Gen Psychiatry. 2006; 63: 1325–35. [PubMed: 17146007]
80. Black J, Kodish I. Pathology of layer V pyramidal neurons in the prefrontal cortex of patients with schizophrenia. Am J Psychiatry. 2004.
81. Huber K. Altered synaptic plasticity in a mouse model of fragile X mental retardation. Proc Natl Acad Sci U S A. 2002.
82. Purpura D. Dendritic spine' dysgenesis' and mental retardation. Science (80-). 1974.
83. Irwin S, Galvez R, Greenough W. Dendritic spine structural anomalies in fragile-X mental retardation syndrome. Cereb Cortex. 2000.
84. Alrahbeni T, Sartor F, Anderson J, Miedzybrodzka Z, McCaig C, Müller B. Full UPF3B function is critical for neuronal differentiation of neural stem cells. Mol Brain. 2015; 8: 33. [PubMed: 26012578]
85. Giorgi C, Yeo GW, Stone ME, Katz DB, Burge C, Turrigiano G, et al. The EJC factor eIF4AIII modulates synaptic strength and neuronal protein expression. Cell. 2007; 130: 179–191. [PubMed: 17632064]
86. Zheng S, Gray EE, Chawla G, Porse BT, O'Dell TJ, Black DL. PSD-95 is post-transcriptionally repressed during early neural development by PTBP1 and PTBP2. Nat Neurosci. 2012; 15: 381–8. S1. [PubMed: 22246437]
87. Colak D, Ji S-J, Porse BT, Jaffrey SR. Regulation of axon guidance by compartmentalized nonsense-mediated mRNA decay. Cell. 2013; 153: 1252–65. [PubMed: 23746841]
88. McBurney MW. P19 embryonal carcinoma cells. Int J Dev Biol. 1993; 37: 135–40. [PubMed: 8507558]
89. Chan W-K, Bhalla AD, Le Hir H, Nguyen LS, Huang L, Gécz J, et al. A UPF3-mediated regulatory switch that maintains RNA surveillance. Nat Struct Mol Biol. 2009; 16: 747–53. [PubMed: 19503078]
90. Lou C-H, Chousal J, Goetz A, Shum EY, Brafman D, Liao X, et al. Nonsense-Mediated RNA Decay Influences Human Embryonic Stem Cell Fate. Stem Cell Reports. 2016; 6: 844–857. [PubMed: 27304915]
91. Metzstein MM, Krasnow MA. Functions of the Nonsense-Mediated mRNA Decay Pathway in Drosophila Development. PLoS Genet. 2006; 2: e180. [PubMed: 17196039]
92. Horiguchi M, Ota M, Rifkin DB. Matrix control of transforming growth factor- function. J Biochem. 2012; 152: 321–329. [PubMed: 22923731]
93. Ng S-Y, Bogu GK, Soh BS, Stanton LW. The long noncoding RNA RMST interacts with SOX2 to regulate neurogenesis. Mol Cell. 2013; 51: 349–59. [PubMed: 23932716]
94. Carter MS, Li S, Wilkinson MF. A splicing-dependent regulatory mechanism that detects translation signals. Embo J. 1996; 15: 5965–75. [PubMed: 8918474]
95. Brar GA, Yassour M, Friedman N, Regev A, Ingolia NT, Weissman JS. High-resolution view of the yeast meiotic program revealed by ribosome profiling. Science. 2012; 335: 552–557. [PubMed: 22194413]

96. Chew G-L, Pauli A, Rinn JL, Regev A, Schier AF, Valen E. Ribosome profiling reveals resemblance between long non-coding RNAs and 5′ leaders of coding RNAs. Development. 2013; 140: 2828–34. [PubMed: 23698349]

97. Guttman M, Amit I, Garber M, French C, Lin MF, Feldser D, et al. Chromatin signature reveals over a thousand highly conserved large non-coding RNAs in mammals. Nature. 2009; 458: 223–7. [PubMed: 19182780]

98. van Heesch S, van Iterson M, Jacobi J, Boymans S, Essers PB, de Bruijn E, et al. Extensive localization of long noncoding RNAs to the cytosol and mono- and polyribosomal complexes. Genome Biol. 2014; 15: R6. [PubMed: 24393600]

99. Smith JE, Alvarez-Dominguez JR, Kline N, Huynh NJ, Geisler S, Hu W, et al. Translation of Small Open Reading Frames within Unannotated RNA Transcripts in Saccharomyces cerevisiae. Cell Rep. 2014; 7: 1858–66. [PubMed: 24931603]

100. Frappart P-O, Lee Y, Lamont J, McKinnon PJ. BRCA2 is required for neurogenesis and suppression of medulloblastoma. EMBO J. 2007; 26: 2732–2742. [PubMed: 17476307]

101. Madabhushi R, Gao F, Pfenning AR, Pan L, Yamakawa S, Seo J, et al. Activity-Induced DNA Breaks Govern the Expression of Neuronal Early-Response Genes. Cell. 2015; 161: 1592–1605. [PubMed: 26052046]

102. Wei P-C, Chang AN, Kao J, Du Z, Meyers RM, Alt FW, et al. Long Neural Genes Harbor Recurrent DNA Break Clusters in Neural Stem/Progenitor Cells. Cell. 2016; 164: 644–655. [PubMed: 26871630]

103. CNV and Schizophrenia Working Groups of the Psychiatric Genomics Consortium CR, Psychosis Endophenotypes International Consortium DP. Merico D, Thiruvahindrapuram B, Wu W, Greer DS, et al. Contribution of copy number variants to schizophrenia from a genome-wide study of 41,321 subjects. Nat Genet. 2017; 49: 27–35. [PubMed: 27869829]

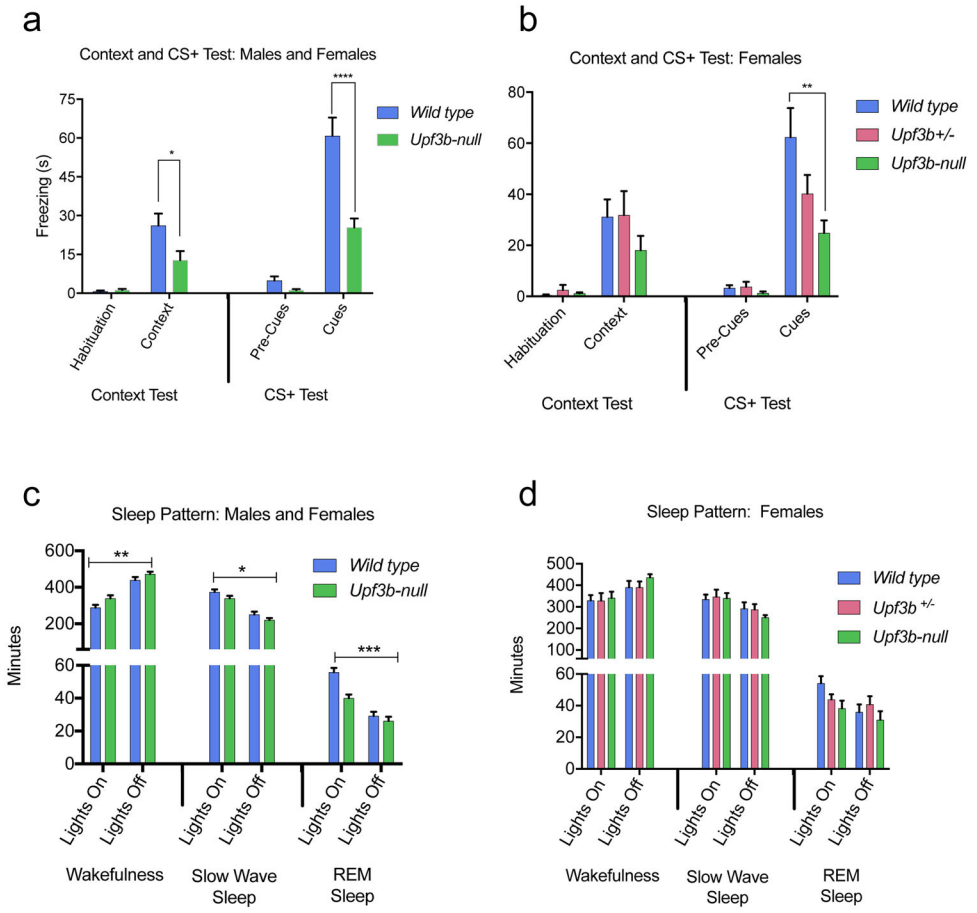

Figure 1.

Upf3b-null mice have cued/contextual fear learning defects and sleep alterations. (**a** & **b**) Measurement of freezing times during habituation periods and after cue introduction and contextual environment introduction in males and females combined (**a**) and females alone (**b**). Analysis of 12 $Upf3b^{-/Y}$ (null) and 13 $Upf3b^{+/Y}$ (control) males; 14 $Upf3b^{-/-}$, 14 $Upf3b^{+/-}$ and 12 $Upf3b^{+/+}$ females. (**c** & **d**) Measurement of time in light and dark environments in wakefulness, slow wave, non-REM sleep in males and females combined (**c**), and females alone (**d**). Analysis of 9 $Upf3b^{-/Y}$ (null) and 9 $Upf3b^{+/Y}$ (control) males; 6 $Upf3b^{-/-}$, 6 $Upf3b^{+/-}$ and 5 $Upf3b^{+/+}$ females. For all panels, statistically significant differences, as measured by a Fisher's PLSD test, are indicated (*p<0.05; **p<0.01; ***p<0.005). Error bars indicate SEM.

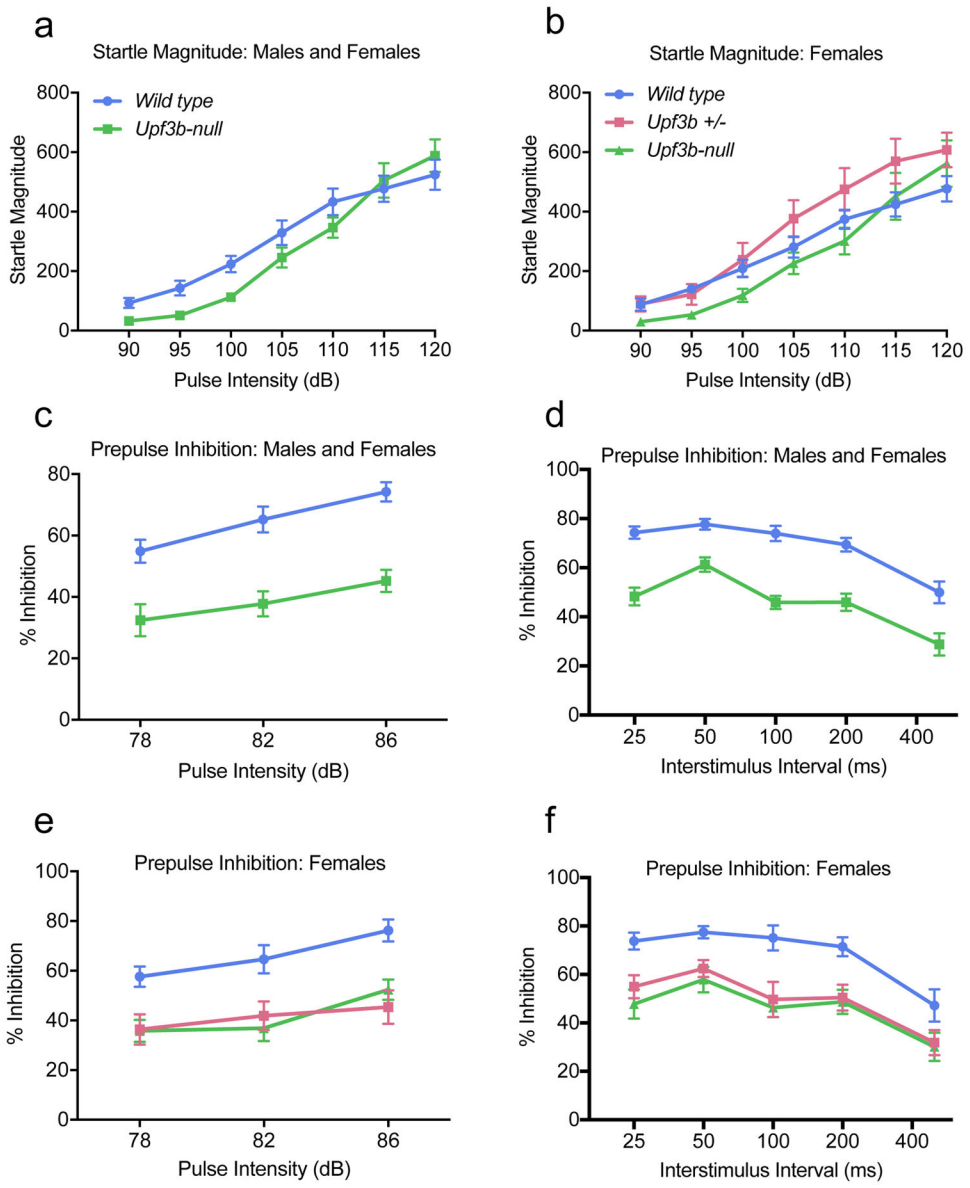

Figure 2.

Upf3b-null display startle and PPI deficits. (**a** & **b**) Measurement of the startle magnitude across different startle pulse intensities in males and females combined (**a**), and females alone (**b**). (**c** & **d**) Prepulse inhibition measured at different prepulse intensities (78 – 86 dB(A) with a 70 dB(A) background) (**c**) or at different prepulse intervals (25 – 500 ms) (**d**) in males and females combined. (**e** & **f**) The same analysis as in panels c and d except that females alone were analyzed. Analysis of 12 $Upf3b^{-/Y}$ (null) and 13 $Upf3b^{+/Y}$ (control) males; 14 $Upf3b^{-/-}$, 14 $Upf3b^{+/-}$ and 12 $Upf3b^{+/+}$ females. Error bars indicate SEM. The text discusses statistically significant effects, as measured by RMANOVA analysis and the Fisher PLSD test.

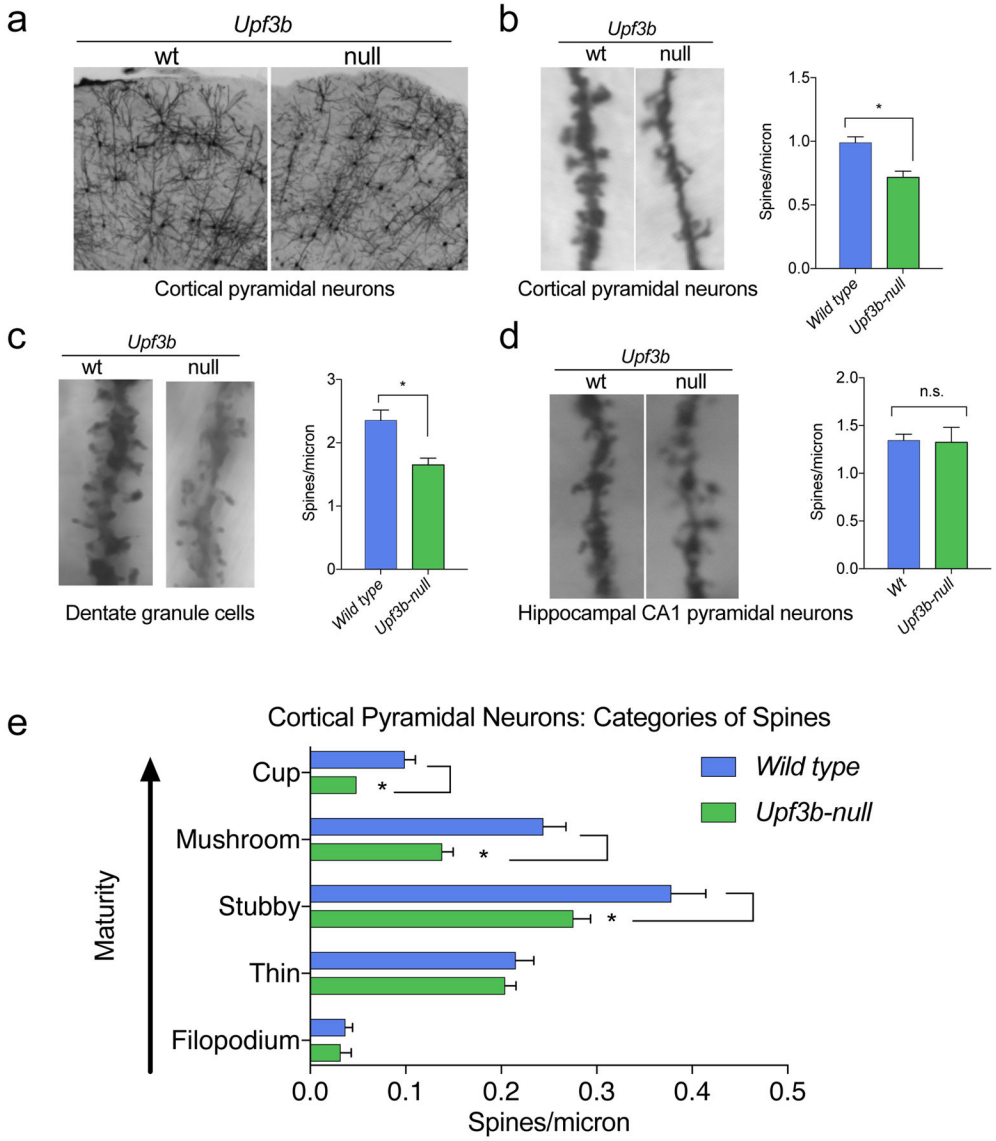

Figure 3.

Dendritic spine analysis in *Upf3b*-null mice. (**a**) Image of prefrontal cortex stained with the Golgi-Cox protocol to reveal neuronal morphology in wild type and *Upf3b*-null mice. (**b–d**) Quantification of dendritic spine density in different neuronal populations in *Upf3b*-null and control brains: pyramidal neurons in the frontal cortex (**b**), granule cells from the dentate gyrus (**c**), and pyramidal neurons in the CA1 region of the hippocampus (**d**). (**e**) Quantification of different categories of spine based on maturation stage between *Upf3b*-null and control pyramidal neurons in the frontal cortex. * denotes statistically significant different values in panels a–e, as judged using the Students T-Test ($p<0.05$; n=3 per genotype). Error bar denote SEM.

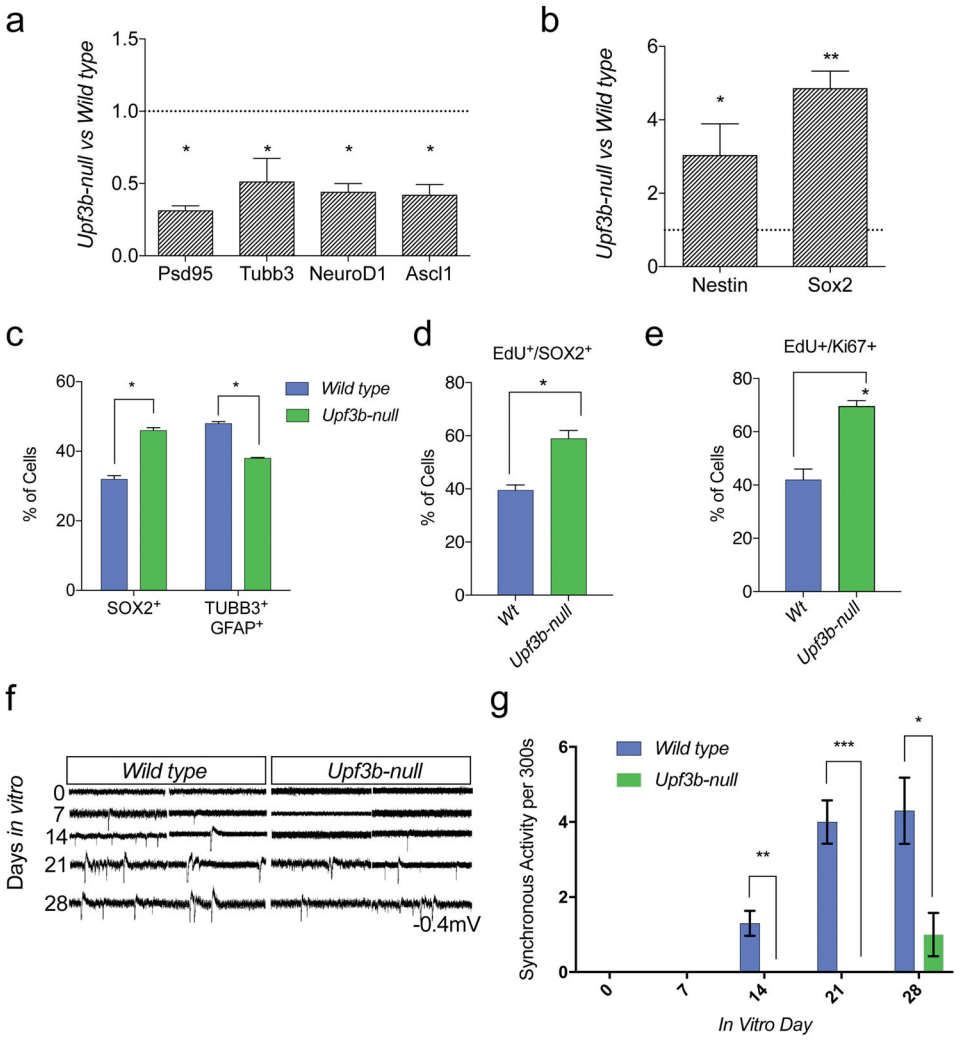

Figure 4.

Upf3b-null NSCs exhibit differentiation defects. (**a** & **b**) qPCR analysis of neuronal differentiation markers (**a**) and NPC markers (**b**) expressed in *Upf3b*-null and control (wild type) mNSC lines cultured for 5 days under differentiation conditions. (**c**) Frequency of cells expressing the NPC marker, SOX2, and the neural differentiation markers, TUBB3 and GFAP, 5 days after differentiation *in vitro.* (**d** & **e**) Frequency of self-renewing mNSC cells, as measured with NPC marker, SOX2 (**d**), or the proliferation marker, KI67 (**e**) and pulse-chase EdU labeling (**d** & **e**). (**f**) Measurement of electrical activity in *Upf3b*-null and control mNSCs differentiated for the days indicated *in vitro*. Each indicated interval is a 20 s window of a 300 s recording. (**g**) Quantification of synchronized firing per 300 s, from experiments performed as in panel f (three independent mNSC lines [each derived from separate embryos] per genotype were analyzed). * denotes statistically significant different values, as judged using the Student's t test ($p<0.05$). Three independent mNSC lines [each derived from separate embryos] per genotype were analyzed. Data points represent mean of biological replicates (n=3 per genotype). Error bars denote standard deviation.

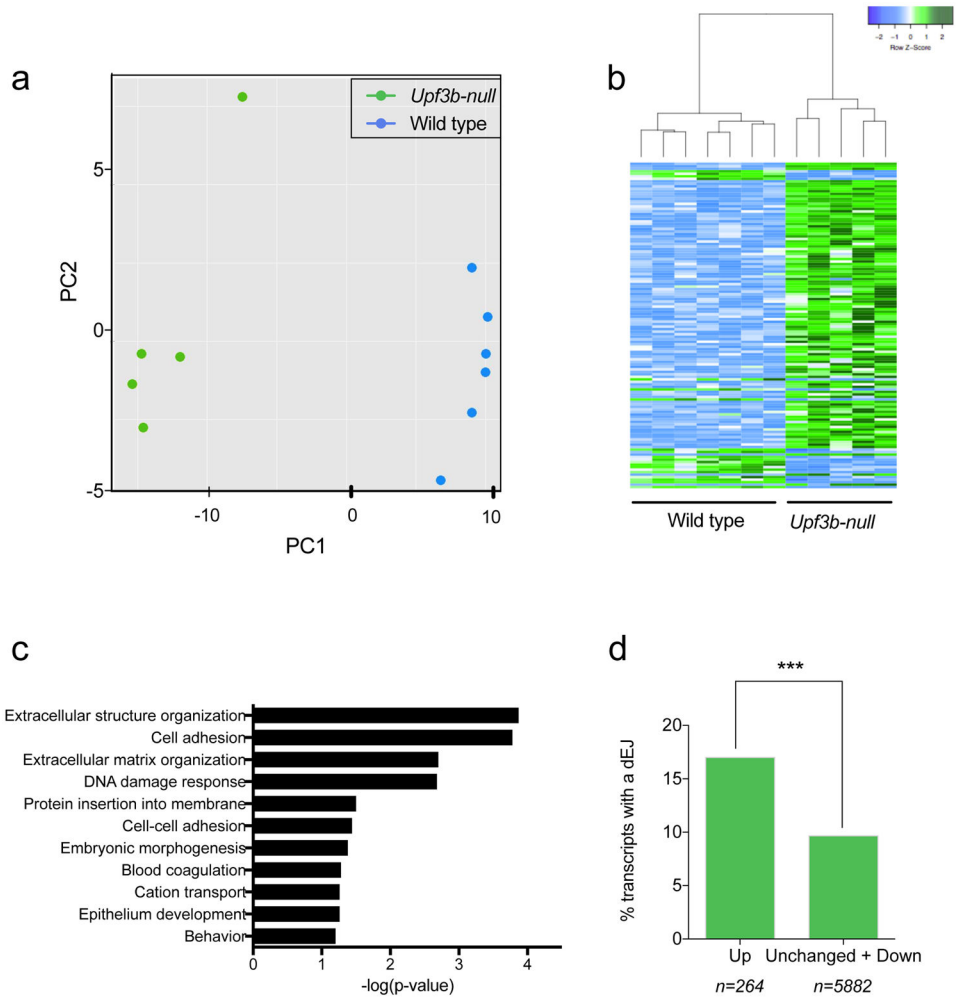

Figure 5.

Identification *Upf3b*-regulated transcripts in the frontal cortex using RNA sequencing. (**a**) Principal component analysis (PCA) of *Upf3b*-null and control frontal cortices (n=5 and 6, respectively), with each point representing a cortex sample from a single mouse. Data was plotted along the first and second principal components. (**b**) Differentially expressed genes in *Upf3b*-null frontal cortex samples compared to wild type controls identified 141 genes upregulated upon loss of *Upf3b* ($q<0.05$, >1.41-fold change). (**c**) Gene ontology analysis of RNAs upregulated upon loss of *Upf3b* in the frontal cortex indicated enrichment for several functional categories. (**d**) The presence of a dEJ was statistically enriched in transcripts upregulated in *Upf3b*-null cortex, as compared to downregulated and unchanged transcripts (Chi-square test; $p<0.0005$). This RNAseq data has been deposited in the GEO DataSets site (GSE99112).

Table 1

NMD-Inducing Features in Neural-Associated UPF3B-Regulated Genes

Gene	dEJ[I]	Long 3′UTR[II]	uORF[III]
Akr1c14	No	Yes	Yes
Arl5c	No	No	No
Brca2	No	No	Yes
Cd59a	No	Yes	Yes
Cdh24	No	No	Yes
Col18a1	No	Yes	No
Dscam	No	Yes	Yes
Dscaml1	Yes	Yes	Yes
Fbn2	No	Yes	No
Hivep3	No	Yes	Yes
Itga8	Yes	Yes	No
Kcnh4	Yes	No	Yes
Mov10	No	No	Yes
Nin	No	No	Yes
Pcdh15	Yes	Yes	Yes
Ptch1	Yes	Yes	Yes
Sdk2	No	Yes	No
Sem4g	Yes	Yes	Yes
Spen	No	Yes	Yes
Tnc	No	No	Yes
Vwa5b1	Yes	Yes	Yes
Rmst	Non-coding RNA		

Genes upregulated in *Upf3b*-null frontal cortex that express at least 1 transcript isoform with the following NMD-inducing features:

[I] exon-exon junction >50 nt downstream of the main ORF

[II] 3′ UTR ≥0.9 kb

[III] at least one uORF with features as described (Shum *et al. Nucleic Acids Res* 43:9314 [2015])